

Thermal Impact of Disk Design on Aircraft Engine Compressor Disks

Syed Naveed Ahmed¹, P Ravinder Reddy², Sriram Venkatesh³

¹PhD Scholar, Mechanical Engineering Department, Osmania University, Hyderabad, Telangana, India

²Professor, Mechanical Engineering Department, CBIT, Hyderabad, Telangana, India

³Professor, Mechanical Engineering Department, Osmania University, Hyderabad, Telangana, India

Abstract- The new generation aircraft engines operate at increased levels of rotational speeds and air temperatures. This results in the rotating compressor disks of the aircraft engine being subjected to high levels of thermal and dynamic stresses. The increased thermal stresses combine with the dynamic stresses to place an upper limit on the useful operating life of these compressor disks. This in effect lowers the reliability thereby demanding more frequent engine checks to be performed by the airline operators as instructed by the engine manufacturer. The result is an increased maintenance cost of these widely used aero engines and a greater down time for the aircraft which effects the overall airline business. In a more extreme scenario it can lead to the premature failure of the compressor disks ahead of the scheduled maintenance thereby effecting the regular flight operations. In view of these stated facts an investigation is carried out to study the thermal impact of the disk design and the flow features over the temperature gradients of the aircraft engine compressor disks. The lowering of the disk temperature gradients achieved by design improvisations would lead to the enhancements in the operating life of these compressor disks. In effect it increases the reliability and lowers the maintenance cost of these widely aero engines. Owing to the complexity of the thermal fluid behavior and the range of inter dependent factors effecting the disk temperatures it is almost impractical to perform experiments for all the possible design configurations. Hence it becomes inevitable to conduct numerical estimations of the disk heat transfer and fluid flow characteristics using computer aided models which are validated with the experimental results. In this study a thermal model of the high speed rotating compressor disks along with flow system is developed with application of Computational Fluid Dynamics (CFD) and Finite Element Analysis (FEA). These computer based thermal models are validated with the experimental results and are used for studying the impact of the disk design and the flow design changes on the compressor disk temperature gradients.

Keywords- Aircraft Engine Compressor Disks, Gas Turbine Compressor Disks, Compressor Disk Design Study, Compressor Secondary Flow Study, Finite Element Analysis, Computational Fluid Dynamics.

Nomenclature

T	:	Temperature, C
ΔT	:	Temperature difference, K
V	:	Flow velocity, m s ⁻¹
d	:	Annulus Gap, m
dh	:	Hydraulic diameter = 2d, m
ν	:	Kinematic viscosity of the fluid, m ² s ⁻¹
r	:	Radius from rotor axis, m
ρ	:	Density of the fluid, kg m ⁻³
μ	:	Dynamic viscosity of the fluid, N s m ⁻²
K	:	Thermal conductivity of air, W m ⁻¹ K ⁻¹
K _{disk}	:	Thermal conductivity of the disk material, W m ⁻¹ K ⁻¹
h	:	Heat Transfer Coefficient, W m ⁻² K ⁻¹
ω	:	Disk angular velocity, rad s ⁻¹
R _b	:	Cavity outer radius, m
R _a	:	Cavity inner radius, m
β	:	Volume expansion coefficient of the fluid, K ⁻¹
RO _{ax}	:	Axial Rossby number
Nu	:	Nusselt Number
Re _{ax}	:	Axial Reynolds Number
Re _{ω}	:	Rotational Reynolds's number
Gr	:	Grashof number
Pr	:	Prandtl number
s	:	Axial width of cavity, m
x	:	Axial distance, m

- Ds : Shaft diameter, m
- m. : Mass flow rate, kg s⁻¹
- xk : Ratio of the air to rotor tangential velocities.
- q : Heat flux, W m⁻²

Subscripts:

- Sh : Shroud
- In : Air inlet to cavity
- Ax : Axial
- Av : Average
- R : At local radius r from axis
- O : Outer
- I : Inner
- Cav : Cavity

I. INTRODUCTION

Figure 1 shows the secondary flow system in the compressor disks region of an aircraft engine. The secondary flow is a certain percentage of the compressor core flow extracted for either heating or cooling the internal parts of the engine in order to reduce the temperature gradients and increase the operating life of these components. But any extraction of the compressor core flow for this secondary application effects the performance of the engine by increasing the specific fuel consumption and lowering the specific thrust. Hence it becomes vital to design the compressor disks and the secondary flow in such a way as to minimize the percentage usage of the core flow for this secondary application and at the same time achieve effective lowering of the temperature gradients in order to maximize the component life. In this research work an investigation is carried out to study the impact of the various disk design and the secondary flow design features on the temperature gradients of the high speed rotating compressor disks. This paper deals with a part of this researchwork and focuses on the investigation of the impact of the disk design features on the compressor disk temperature gradients.

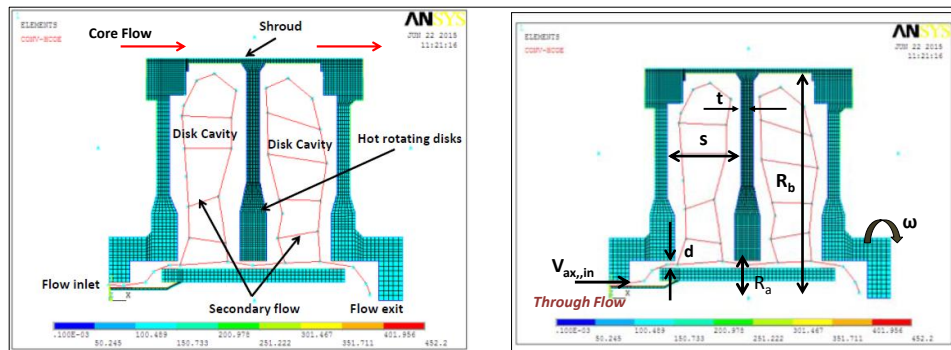


Fig.1 The rotating compressor disks and the secondary flow with the nomenclature

Most of the earlier research in this field deals with the metal to fluid interactions of the secondary flow with the rotating compressor disks using experimental setups. Also these experimental investigations are confined to a particular region of the rotating compressor disks and do not address the broader issue of the impact caused by the changes in the disk design and the secondary flow design on the temperature gradients experienced by the compressor disks. To quote a few examples, the experimental works done by Farthing et al. [3,4], Gunther et al. [1], Long [15], Michael et al. [16] were focused on the heat transfer studies limited to the rotating cavities of the compressor disks. The experimental works done by Long et al. [13] and Reby et al. [14] addresses heat transfer phenomenon limited to the shroud regions of the rotating cavities of the compressor disks.

On the contrary in this work a broader study of the complex heat transfer phenomenon occurring within the secondary flow system is carried out using numerical estimations and the impact of the various disk design and the flow design features on the temperature gradients of the rotating compressor disks is estimated and analysed. As stated earlier this paper highlights a part of this study which deals with the estimations of the impact of the disk design on the temperature gradients of the rotating compressor disks. Also owing to the complexity of the thermal fluid behavior and the range of inter dependent factors that affect the disk temperatures it becomes impractical to perform experiments over all the possible range of design parameters. Hence it becomes inevitable to conduct

numerical estimations of fluid flow and heat transfer after these numerical models have been duly validated with the experimental results. The current investigation is carried out by simulating the flow and heat transfer characteristics using Computational Fluid Dynamics (CFD) and Finite Element Analysis (FEA). These computer models used for the thermal simulations and for investigating the impact of the disk design on the disk temperature gradients are validated with the experimental results.

In this study the following features of the disk design are selected to investigate the thermal impact on the rotating compressor disks.

The disk material.

The disk thickness (t).

The axial Rossby number (RO,ax)

The axial gap ratio (G).

The axial Rossby number is the ratio of the flow axial velocity to the disk rotational speed at the radius where the flow enters the rotor cavity (Figure 1).

$$RO_{ax} = V_{ax,in} / \omega R_a \tag{1}$$

The axial gap ratio is the ratio of the axial gap between the adjacent disks to the outer radius of the disk cavity (Figure 1).

$$G = s / R_b \tag{2}$$

The variations in the disk and flow design alter the heat transfer and the fluid flow characteristics of the secondary flow through the compressor disk cavities (Figure 1). These design changes cause a parametric impact on some or all of the following factors in the secondary flow system.

The flow structure within the rotating disk cavities.

The swirl velocities of the re-circulating flows inside the rotating disk cavities.

The pressure and density of the flow inside the rotating disk cavities.

The convective heat transfer coefficients at various convection zones in the secondary flow system.

The rate of heat generation in the rotating disk cavities.

The study focuses on estimating the parametric impact of the design changes on the various factors listed above from a) to e) in the secondary flow system and the ultimate impact on the compressor disk temperature gradients.

This investigation is carried out using the computer aided numerical models which are validated with the experimental results.

II. THE FEM MODEL AND CFD SIMULATION

Figure 2 represents the experimental set up and the Finite Element Model (FEM) built in Ansys for studying the secondary flow heat transfer and the thermal impact of the disk design on the rotating compressor disks. The thermal model is developed from the geometric configuration and the operating conditions of the experimental work [1].

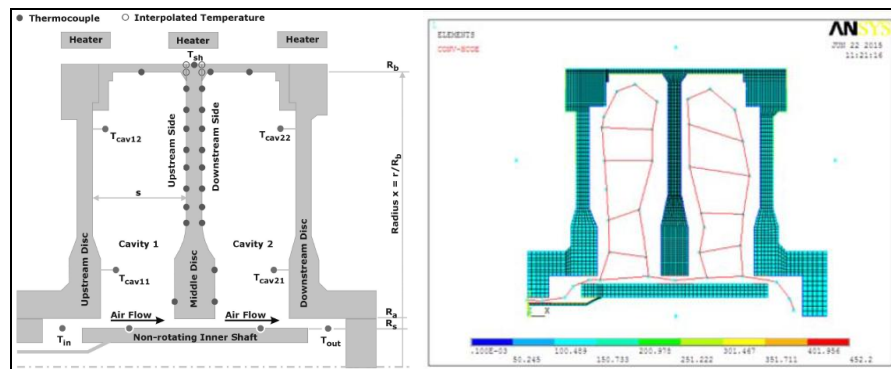


Fig. 2. The experimental set up and the Ansys model

The Finite Element model developed in Ansys is a thermal axis symmetrical model, with Plane 55, Surf 151 and Fluid 116 elements. The Ansys model is run for two operating conditions of the experimental set up a) Test and measurement conditions and b) Maximum test rig conditions. The model is then validated against the experimental results obtained for the “test and measurement conditions” before being used for studying the thermal impact of the axial Reynolds number.

Table 1 shows the two operating conditions at which the engine is operated.

Table .1 The two operating conditions of the engine

	ΔT	Re_{ax}	Re_{ω}	Gr	$Ro_{,ax}$	\dot{m}	N
	K					kg/s	r.p.m
<u>Measurement Test conditions</u>	70	2×10^4	1.5×10^6	6×10^{11}	1	0.04	6000
<u>Maximum test conditions</u>	70	1.8×10^5	1.5×10^7	5×10^{13}	1	0.4	12000

Where : ΔT is the difference between the disk shroud temperature and the inlet air temperature. $\Delta T = T_{sh} - T_{in}$ (3)

Gr is the Grashof number and Re_{ω} is the Rotational Reynolds's number

$Ro_{,ax}$ is the Axial Rossby number given by $Ro_{,ax} = V_{ax, in} / \omega Ra$ (4)

Re_{ax} is the axial Reynolds number. $Re_{ax} = V_{ax, in} dh / \nu$ (5)

Which is a non-dimensional representation of the mass of the secondary flow entering the rotor cavity.

Ra is the cavity inner radius, $V_{ax, in}$ is the axial flow velocity at cavity inlet and dh is the hydraulic diameter which is twice the annulus gap "d" (Figure 1).

For building the flow structure in Ansys which closely represents the actual secondary flow a CFD model is built in Gambit and Fluent. In addition to building the flow structure the CFD results are used to estimate the pressure and swirl velocity variations which are subsequently used to estimate the convective heat transfer coefficients and the heat generation inside the rotating cavities. The CFD model is an axis symmetric model with compressible flow and uses Spalart-Allmaras equation for the viscous flow solution.

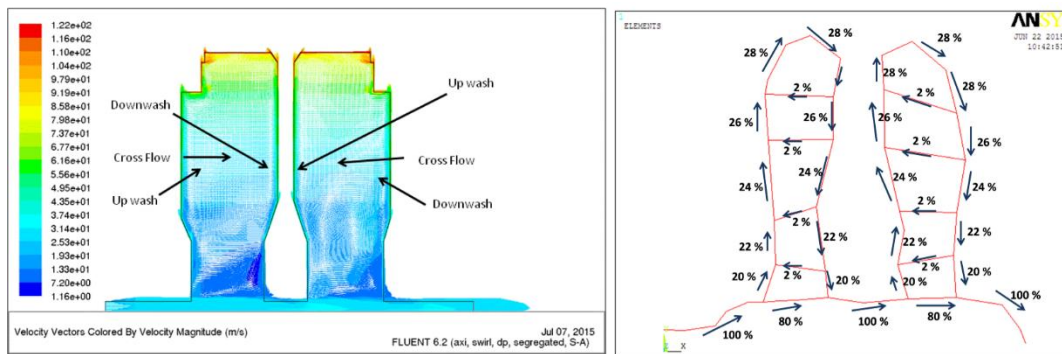


Fig. 3. Flow vector pattern in Fluent and the percentage flow recirculation

Based on the flow vector patterns obtained from Fluent the flow network inside the cavities is built in Ansys (Figure 3). An estimated 20 per cent of the flow circulates into the inter disk cavity with 2 per cent local re circulations. For test conditions 100 per cent flow corresponds to 0.04 Kgs/sec and for maximum test rig conditions corresponds to 0.4 Kgs/sec.

III. VALIDATION OF THE THERMAL MODEL WITH EXPERIMENTAL RESULTS

The estimated thermal boundary conditions and flow re circulations are applied on the Ansys model to obtain the temperature distributions over the rotating compressor disks. The details of the methodology of estimating the thermal boundary conditions is discussed in detail in the sections to follow. The Ansys thermal model with the estimated boundary conditions is validated with the experimental results of the "test and measurement conditions" (Table 1).

During the experimental work [1] the thermal data is obtained for the middle disk while operating the engine at the "test and measurement conditions" (Table 1). The thermal model is validated with the experimental results bycomparing theradial heat flux data across the mid-section of the rotating disk (Figure 4). The radial heat flux on

the disk is selected for the model validation purpose as it influences the radial temperature gradients which dictate the useful life of the rotating compressor disks. The radial heat flux through the disk is given by equation 7.

$$q_{radial} = -K_{disk} \frac{dt}{dr}, \tag{7}$$

where dt/dr is the temperature gradient over the middle of the disk (Figure 4) in the radial direction.

Figure 5 shows the comparison of the estimated radial heat fluxes from Ansys (analytical) with the radial heat fluxes obtained from the experiment [1] through the mid-section of the middle disk (Figure 4) from its inner to the outer radius. The vertical scale of the plot represents the disk local radius r which is normalized with the disk outer radius R .

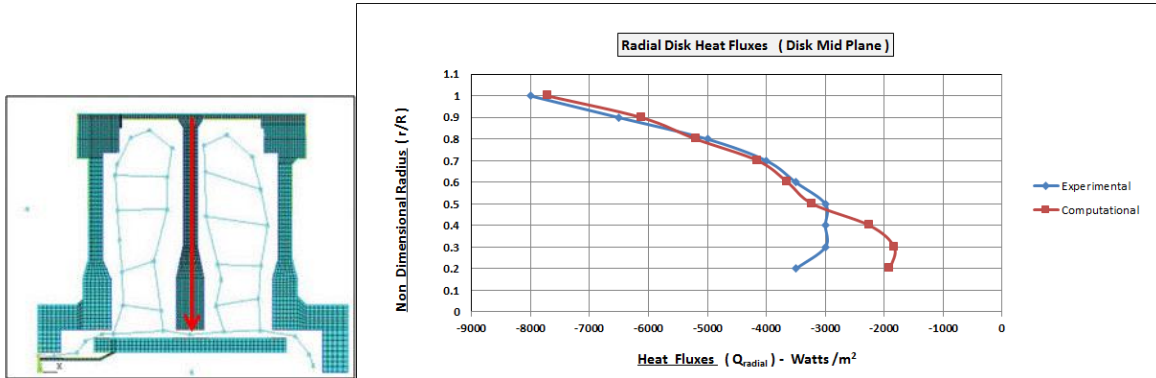


Fig.4 Region where radial heat fluxes are compared Fig.5. Comparison of radial heat fluxes of the analytical model with the experiment

As seen from this comparison (Figure 5) the estimated radial heat fluxes from the analytical model are in close agreement with the experimental results (within 10 per cent) except for the very inner radial locations of the disk. This deviation at the very inner radial locations of the disk is due to the sudden change in the disk thickness which gives an experimental error as mentioned in the experimental study. The outer and middle regions of the disk are critical in terms of studying the temperature gradients as they are the ones which dictate the operating life of these disks and as seen from figure 5 these regions are in very close agreement with the experimental results. The thermal model which is validated with the experimental results is used to investigate the impact caused by the changes in the disk design over the temperature gradients of the rotating compressor disks.

IV. ESTIMATION OF THE CONVECTIVE HEAT TRANSFER COEFFICIENTS

The heat transfer between the rotating compressor disks and the secondary flow is strongly influenced by the convective heat transfer coefficients across the various zones of the compressor as highlighted in figure 6. These convective heat transfer coefficients depend on various factors determined by the design of the disks, the design of the secondary flow system and the operating conditions of the engine. The selection of the heat transfer correlations and the estimation of the convective heat transfer coefficients over these various zones (Figure 6) is discussed in the sections that follow (sections 4.1 to 4.6).

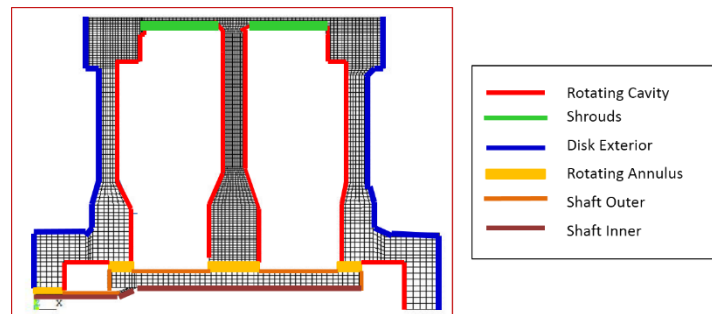


Fig. 6. The convection heat transfer zones

Figures 7 to 9 show the convective heat transfer coefficients estimated over the various heat transfer zones (Figure 6) for the two operating conditions of the engine.

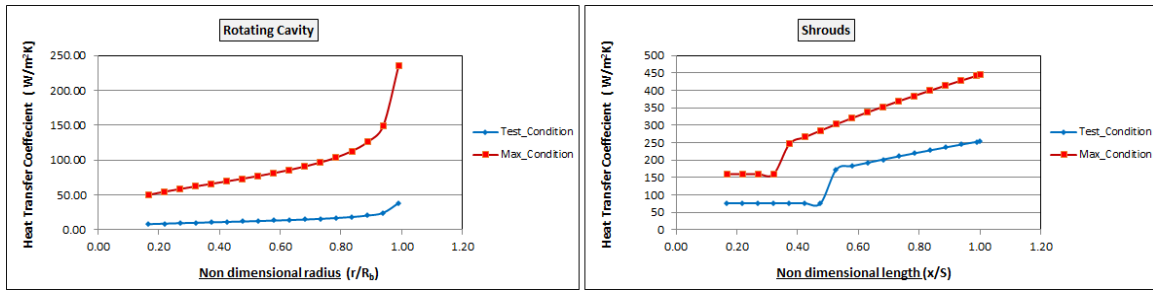


Fig. 7. Estimated convective heat transfer coefficients on the rotating cavity and the shrouds for the two operating conditions.

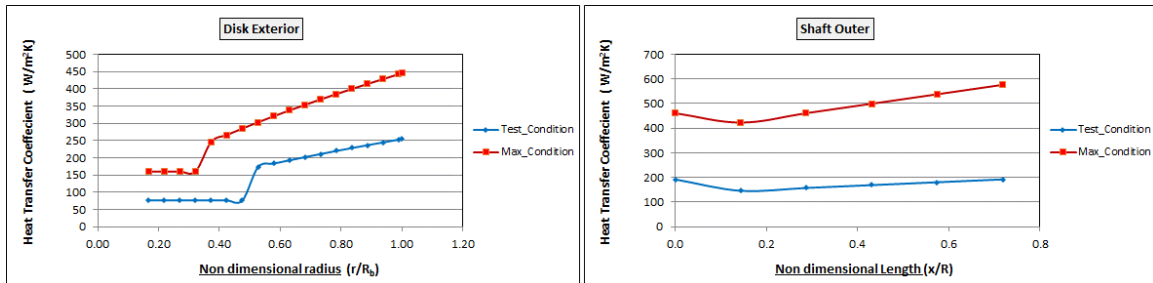


Fig. 8. Estimated convective heat transfer coefficients on the disk exterior and the shaft outer for the two operating conditions.

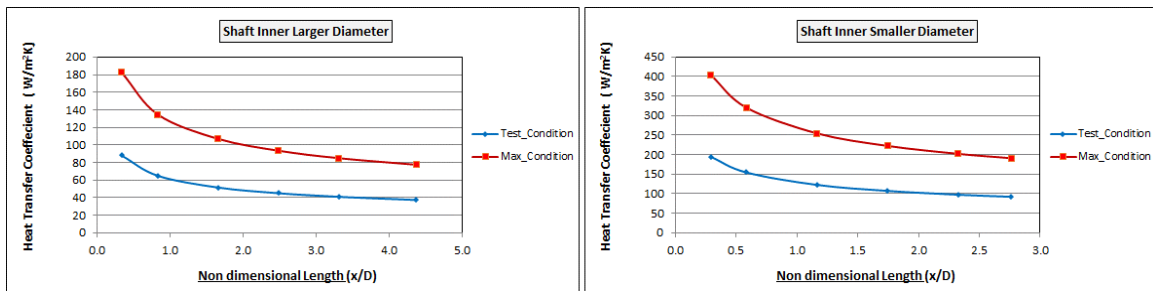


Fig. 9. Estimated convective heat transfer coefficients on the shaft inner for the two operating conditions.

4.1 Estimation of the Convective Heat Transfer Coefficients in the Disk Rotating Cavities:

The following correlation (equation 8) is selected for estimation of the convective heat transfer coefficients in the disk rotating cavity (Figure 6). The correlation is based on the experimental work done by Farthing et al. [3,4]. The data from the experiment was used to fit into an equation that actually represents laminar natural convection over a vertical plate, given by

$$Nur = 0.0054 Re_{ax,in}^{0.3} Gr^{0.25} (x-1 - 1)^{-0.25} \tag{8}$$

Where Nur , Gr are the local Nusselt, Grashof numbers at a certain radius from the disk.

$$Re_{ax,in} \text{ is the axial Reynolds number at the inlet to the disk cavities} = \rho_{in} V_{ax,in} dh / \mu_{in} \tag{9}$$

Where dh is the hydraulic diameter based on the gap at the flow inlet between the disk inner and the shaft (Figure 2).

x is the non dimensional radial coordinate = r / Rb, based on cavity outer radius.

In equation 8, the axial Reynolds number represents the extent of impact of the axial through flow mixing with the buoyancy induced flow in the cavity on the convective heat transfer. The Grashof number represents the strength of the buoyancy induced flows in the cavity based on the rotational speed of the disk (ω) and the air temperature difference (ΔT). As seen from this equation the heat transfer in rotor cavity is mostly dominated by the buoyancy induced flow in terms of the Grashof number with less impact of the mixing of axial flow with cavity flow circulations.

The convective heat transfer coefficients estimated inside the disk rotating cavities for the two engine operating conditions is shown in figure 7. The horizontal scale (Figure 7) represents the disk local radius r which is normalized with the disk outer radius R_b .

4.2 Estimation of the Convective Heat Transfer Coefficients in the Shroud Region:

The heat transfer in the shroud region (Figure 6) is governed by the mechanism of free convection. This is because at larger radius of the rotor cavity, the effects of axial through flow are very weak. As a result, a quasi-solid body rotation occurs and the effects of buoyancy are expected to be strong. Hence the heat transfer at the larger radii of the cavity near the shroud is due to free convection generated by the buoyancy induced flow. It is hence recommended that a correlation be used which captures the effect of free convection in a field effected by gravitational forces.

In an engine during the acceleration and the steady state conditions, the shroud is relatively hotter than the disks. Long and Tucker [13] reported on heat transfer measurements from the shroud. They have stated that the disk surface temperature distribution appears to have little effect on the shroud heat transfer and that the shroud heat transfer is in a reasonably good agreement with an established correlation for free convection from a horizontal surface. The following correlations (equations 10,11) are selected for the estimation of the convective heat transfer coefficient in the shroud region. They are based on the study carried out by Lloyd and Moran [8] on a horizontal plate with upper surface heated and lower surface exposed to free convection along with the gravitational effects as is the case of the shroud in the rotor cavity.

For laminar conditions, $Gr_{sh} < 107$: The shroud Nusselt number $Nu_{sh} = 0.54 (Gr_{sh} Pr)^{1/4}$ (10)

For turbulent conditions, $Gr_{sh} > 107$: The shroud Nusselt number $Nu_{sh} = 0.15 (Gr_{sh} Pr)^{1/3}$ (11)

Where : Shroud Grashof number $Gr_{sh} = \rho \omega^2 R_b \beta \Delta T_{sh,av} (s/2)^3 / \mu \nu^2$ (12)

The heat transfer between the shroud and the circulating flow is governed by the buoyancy forces influenced by the disk rotational speeds (ω) and the air temperature gradients (ΔT) inside the disk cavity. The effects of these buoyancy forces on the shroud heat transfer are captured by the Grashof number (equation 12). The air properties used in these equations are based on the condition of air at the cavity inlet. The Grashof number estimated in the shroud region for our study case indicates that the flow around the shroud is turbulent in nature and hence the heat transfer is governed by the equation 11.

The convective heat transfer coefficients estimated over the rotating shrouds for the two engine operating conditions is shown in figure 7. The horizontal scale (Figure 7) represents the axial distance x on the shroud which is normalized with the width of the cavity s .

4.3 Estimation of the Convective Heat Transfer Coefficients Over the Disk Exterior:

The heat transfer over the exterior of the disks (Figure 6) is modelled as a disk rotating in quiescent air. The flow characteristics over a rotating disk is strongly dependent on the local rotational Reynolds number at a certain radius given by

$$Re_r = \omega r^2 / \nu \quad \mu \nu^2 \quad (13)$$

The research on convective heat transfer over rotating disks has been carried out by many authors. According to their findings, the heat transfer over the surface is also affected by the radial temperature profile. Authors usually correlate the local and mean Nusselt numbers by power laws. These correlations are listed in the published literature by S. Harmand, J. Pelle [7]. The power law for both laminar and turbulent regions is given by the local Nusselt number (equation 13) and the averaged Nusselt number (equation 14).

$$Nu_r = a Re_r^b \quad \text{and } Nu_{R,av} = c Re_R^d \quad (14)$$

Where Re_r is the local rotational Reynolds numbers at a radius r from the disk rotational axis, $Re_r = \omega r^2 \rho / \mu$ (15) and Re_R is the rotational Reynolds number at the external radius R , from the disk rotational axis, $Re_R = \omega R^2 \rho / \mu$ (16)

The coefficients a , b , c and d are a function of the type of flow regime (range of Reynolds number), the disk's radial temperature distribution and the Prandtl number.

Up to the radius where the flow is laminar Reynolds number less than 3.6×10^5 , the heat transfer coefficient is estimated based on the averaged Nusselt number given by $Nu_{R,av} = a Re_R^{0.5}$, where R is the radius at which the laminar region ends. The constant $a = 0.261 (n + 2)^{0.5}$ where n is based on the disk temperature profile and in our case is equal to 1. For the outer regions of the disk where the flow is turbulent that is for Reynolds number greater than 3.6×10^5 , the heat transfer coefficient is based on the local Nusselt number given by $Nu_r = a Re_r^b$, where r is the local radius of the disk in the turbulent region from the axis of rotation. The exponential b is equal to

0.8. As in case of the laminar flow the coefficient “a” is effected by the disk temperature profile and given by $a = 0.0162 (n + 2.6)^{0.2}$, where n is based on the disk temperature profile and in our case is equal to 1.

For the operating conditions under study a combination of both the laminar and turbulent conditions exist over the exterior of the disk. As the rotational speed of the disk rises the region of turbulent conditions on the disk exterior increases enhancing the convective heat transfer from disk to the outside air.

The convective heat transfer coefficients estimated over the exterior of the disk for the two engine operating conditions is shown in figure 8. The horizontal scale (Figure 8) represents the disk local radius r which is normalized with the disk outer radius Rb. The sudden spike in the convective heat transfer coefficient at around 50 per cent disk radius is due to the fact the flow turns from laminar to turbulent at this point.

4.4 Estimation of the Convective Heat Transfer Coefficients Inside the Rotating Annulus:

The following correlation (equation 17) is selected for estimation of the convective heat transfer coefficients in the cavities of the rotating annulus (Figure 6). The correlation is based on the experimental work done by S. Seghir-Ouali [5]. The data from the experiment was used to fit into an equation given by

$$Nu = 0.01963 Re_{ax}^{0.9285} + (8.5101 \times 10^{-6}) Re_{\omega}^{1.4513} \tag{17}$$

Nusselt Number is based on the annulus gap, $Nu = hd / k$ (18)

Axial Reynolds Number inside Annulus $Re_{ax}(Annulus) = \rho V_{ax}(Annulus) d / \mu$ (19)

Rotational Reynolds Number inside annulus $Re_{\omega}(Annulus) = \rho \omega d^2 / \mu$ (20)

Where, $V_{ax}(Annulus)$ is axial flow velocity inside annulus, d is the annulus gap and ω is the angular speed of the rotor.

The heat transfer coefficients obtained from the above correlation (equation 17) are checked by applying the experimental curves obtained by Gazley [6] who obtained the experimental data using a long rotating cylinder in a concentric stationary cylinder. The former results were in good agreement with the latter results. As seen in equation 17, the heat transfer in the annulus region is influenced by the combined effect of the flow axial velocity through the annulus and the rotational speed of the compressor disk. The convective heat transfer coefficients estimated in the annulus regions for the two engine operating conditions is shown in tables 3 and 4.

Table .2 Heat transfer coefficient for test and measurement conditions

Re_{ax}	Re_{ω}	Nu	h
Axial Reynold Number	Rotational Reynold Number	Nuselt Number	Heat Transfer Coefficient (w / m ² k)
1.00E+04	1.44E+03	101.9	452.2

Table .3 Heat transfer coefficient for maximum test rig condition

Re_{ax}	Re_{ω}	Nu	h
Axial Reynold Number	Rotational Reynold Number	Nuselt Number	Heat Transfer Coefficient (w / m ² k)
9.00E+04	1.44E+04	791	3508

4.5 Estimation of Convective Heat Transfer Coefficients Over the Shaft Outer:

The heat transfer over the outer face of the shaft (Figure 10) is closely modelled as an axial flow over a cylinder. Although there exists a good number of experimental studies that give information about the Nusselt number variations over single cylinders in cross flow, there is very limited information for cylinders with axial flow. In the experimental work, carried out by Roland Wiberg [11] heat transfer studies were conducted for axial flow over cylinders. Measurements were made for the Nusselt number and temperature distribution over the cylinder for two configurations. A) Cylinder with low upstream turbulence B) Cylinder with an upstream flow affected by turbulence. The latter configuration was selected for the estimation of the convective heat transfer coefficients over the non- rotating shaft. The initial turbulence at the entry of the shaft is due to the flow coming out from the annulus.

Correlations were developed by Roland Wiberg [11] for axial flow over cylinders correlating the Nusselt numbers with the Reynolds numbers. The subsequent results were plotted (Figure 11) for the averaged Nusselt numbers over the front, the middle and the rear faces of the cylinder, for varying Reynolds numbers. The ranges a to b, b to c, c to d, on the horizontal scale (Figure 11) refer to the front face, the cylindrical face and the rear face of the shaft in terms of the length “x” measured from the flow entrance, which is made non-dimensional with respect to the shaft radius R.

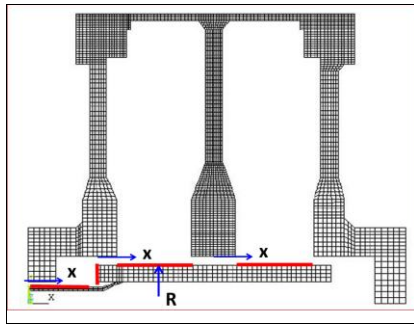


Fig. 10 Convection zones on Shaft outer faces

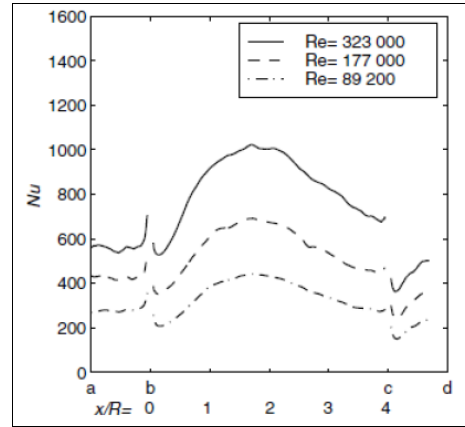


Fig. 11. Experimental curves of Nusselt number

The Nusselt numbers over the shaft (Figure 10) are estimated by using the experimental curves (Figure 11). The convective heat transfer coefficients are then estimated based on these Nusselt number equation given by $Nu = h D_s, 0 / k_{in}$ (20)

The convective heat transfer coefficients estimated over the shaft outer for the two engine operating conditions is shown in figure 8. The horizontal scale (Figure 8) represents the distance x on the shaft from the flow entrance which is normalized with the shaft radius R.

4.6 Estimation of the Heat Transfer Coefficients Inside the Engine Shaft:

The heat transfer inside the shaft (Figure 6, shaft inner) is modelled as internal flow through ducts using equation 21 which is a standard correlation used for ducts with shorter lengths having $(L x / D_{s,i}) / Re_{ax,duct} Pr < 0.01$ and the reference can be found in the Heat and Mass Transfer Data book [9].

$$Nu = 1.67 [Re_{ax,duct} Pr / (x / D_{s,i})]^{0.333} \tag{21}$$

In this study, $D_{s,i}$ refers to the shaft inner diameter and L to the shaft length.

$Re_{ax,duct}$ refers to the Reynolds number of the shaft internal flow

x is the distance measured from the flow entrance to the shaft

The heat transfer correlation 21 is used to evaluate the local convective heat transfer coefficients on the inside of the shaft with both the larger diameter ($Re_{ax,duct} = 1 \times 10^5$) and the smaller diameter ($Re_{ax,duct} = 1.76 \times 10^5$). The sections of the shaft inner with larger and smaller diameters are shown in figure 6.

The convective heat transfer coefficients estimated on the shaft inner for the larger and the smaller diameters for the two engine operating conditions is shown in figure 9. The horizontal scale (Figure 9) represents the distance x on the shaft from the flow entrance which is normalized with the shaft diameter D.

V. ESTIMATION OF HEAT GENERATION IN THE ROTOR CAVITIES

As the air flows and circulates in the inter disk spaces (Figure 12) it forms a forced vortex and interacts with the rotating disks either gaining or losing heat. The heat generations resulting from this work interactions between the flow and the rotor eventually impacts the temperature gradients on the rotating compressor disks. The results from the CFD indicate that the flow moves outwards (outward pumping) towards the left of the inter disk spacing and inwards (inward pumping) towards the right of the inter disk spacing (Figure 12).

The heat generations inside the inter disk spacing is estimated using the Euler’s work equation (22) for the forced vortex flow.

$$Q = m_{cav} \omega^2 [x_{k2} r_{22}^2 - x_{k1} r_{12}^2] \tag{22}$$

Where, m_{cav} is the mass flow through the cavity inside the disk spacing

ω is the angular velocity of the rotor

r_1, r_2 are the inner and outer radii of the cavity
 xk_1 is the ratio of the air to rotor tangential velocities at flow entry to the cavity.
 xk_2 is the ratio of the air to rotor tangential velocities at flow exit to the cavity.
 The ratios of the air to rotor tangential velocities (xk_1, xk_2) are estimated based on the CFD results obtained for the two engine operating conditions (Table 1). The mass flow rate (m_{cav}) through each cavity is based on the flow circulations estimated from the CFD study.

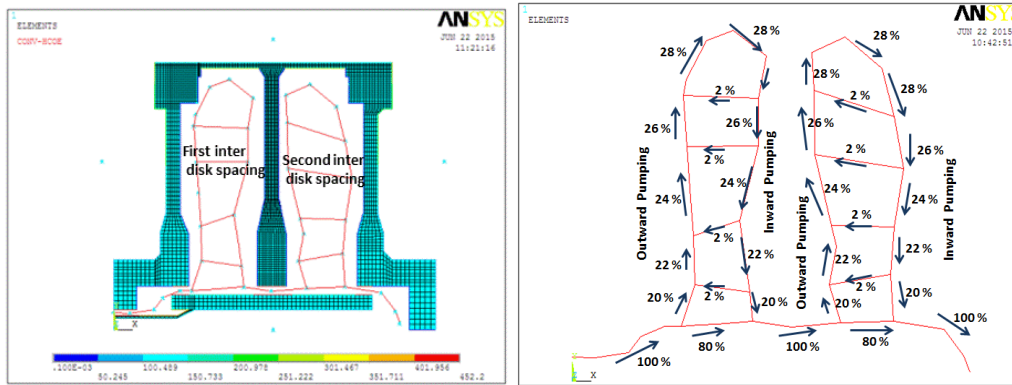


Fig.12. The inter disk spacing and the flow re circulations within these inter disk spacing

The first inter disk spacing (Figure 12) is divided into a total of 15 cavities for estimation of the heat generations. During the outward movement (pumping) of air in the first disk spacing the flow passes through cavities numbered from 4 to 11. During its inward movement (pumping) in the first disk spacing the flow passes through cavities numbered 12 to 18. Likewise the second inter disk spacing (Figure 12) is divided into a total of 13 cavities for the estimation of the heat generations. The size of these cavities depend on the length of the flow vectors constructed in the Ansys model. The magnitude of the heat generation depends on the cavity size, the mass flow through each cavity and the increase in the tangential component of the flow velocity as the flow enters and leaves the cavity. Figure 13 represents the heat generations estimated during the outward and the inward pumping of the flow through these cavities in the first inter disk spacing for the two operating conditions of the engine (Table 1). The positive values of heat generations represent the heat flow from the rotating disks to the circulating air and the negative values represent the vice versa.

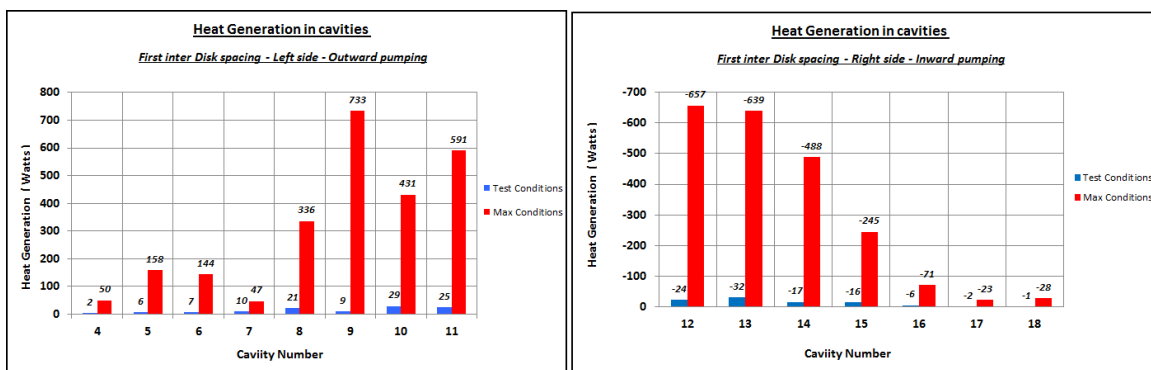


Fig.13 Heat generations in the first inter disk spacing for the outward and the inward pumping.

VI. IMPACT OF THE DISK MATERIAL ON THE DISK TEMPERATURE GRADIENTS

The Ansys thermal model which is validated with the “Test and Measurement Conditions” (Table 1) is used to investigate the impact caused by the variations in the disk thermal conductivity on the disk temperature gradients. The disk thermal conductivity is varied between 30 to 90 percent starting from a minimum 11 W/m K to a maximum of 21 W/m K.

Figure 14 shows the temperature distribution on the rotating compressor disks obtained from Ansys for the minimum ($K = 11$ W/m K) and the maximum ($K = 21$ W/m K) thermal conductivities under study.

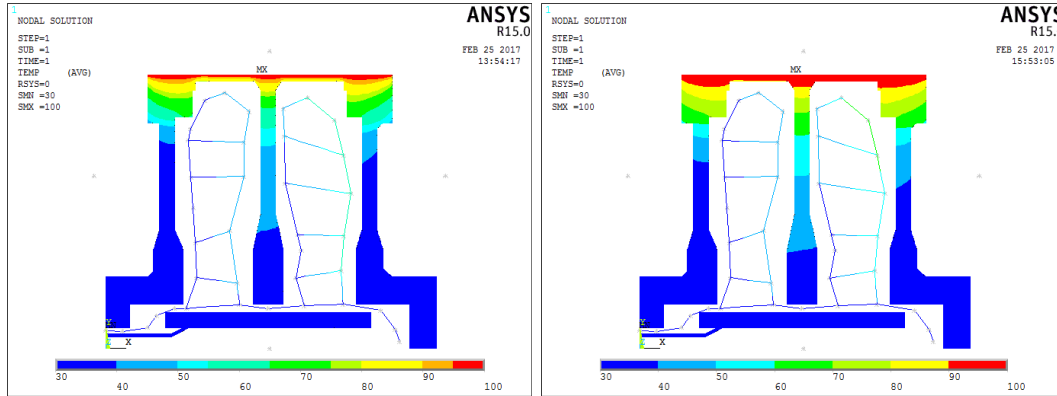


Fig.14 Ansys plot of temperature distribution for the minimum ($K = 11 \text{ W/m K}$) and the maximum ($K = 21 \text{ W/m K}$) thermal conductivity.

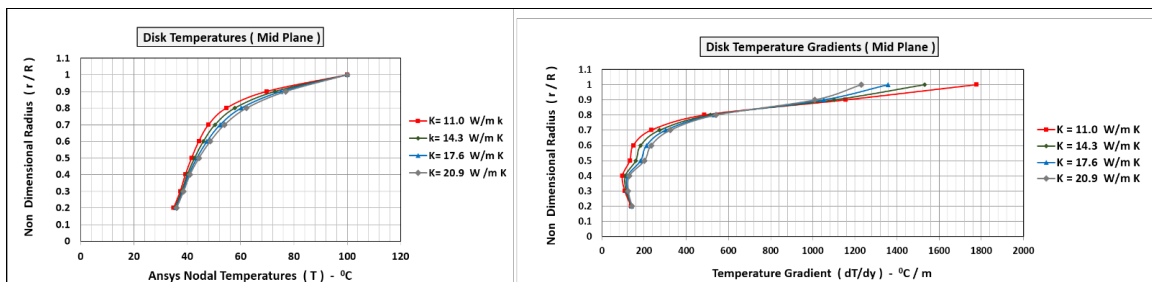


Fig.15 Impact of disk thermal conductivity on disk temperatures and disk temperature gradients

Figure 15 shows the temperatures and the temperature gradients along the mid-section (Figure 4) of the rotating compressor disk for the range of thermal conductivities under study. The vertical scale of the plot represents the disk local radius r which is normalized with the disk outer radius R . The horizontal scale represents the disk nodal temperatures and disk nodal temperature gradients estimated using the Ansys simulation. Tables 4 and 5 show the percentage change in disk temperatures and disk temperature gradients estimated at different radial locations of the disk as the thermal conductivity is raised from the minimum ($K = 11 \text{ W/m K}$) to the maximum ($K = 21 \text{ W/m K}$).

Table .4 Impact of thermal conductivity on disk temperatures

Disk Radial Location (r/R)	Disk Temperature $^{\circ}\text{C}$		% change in temperature
	$K = 11 \text{ W/m}^2 \text{ K}$	$K = 20.9 \text{ W/m}^2 \text{ K}$	
0.2	35	36	3
0.4	39	41	5
0.6	44	49	11
0.8	55	62	13
0.9	70	77	10

Table .5 Impact of thermal conductivity on disk temperature gradients

Disk Radial Location (r/R)	Disk Temperature Gradient $^{\circ}\text{C/m}$		% change in Temperature Gradient
	$K = 11 \text{ W/m}^2 \text{ K}$	$K = 20.9 \text{ W/m}^2 \text{ K}$	
0.2	139	142	2
0.4	98	130	33
0.6	149	233	56
0.8	486	541	11
0.9	1157	1010	-13

As observed from the Ansys plot (Figure 14) and the plotted results (Figure 15) the increase in the thermal conductivity raises the disk temperatures across all the regions of the rotating disk. Also as noted from the table of results (Table 4) the temperatures over the middle and outer regions of the disk ($r/R > 0.5$) are more sensitive to changes in the thermal conductivity compared to the inner regions ($r/R < 0.5$) of the rotating disk. At 20 percent of the disk radius ($r/R = 0.2$) the increase in temperature is 3% compared to 10% at the disk outer radius ($r/R =$

0.9).The higher sensitivity of the disk towards it’s outer regions ($r/R > 0.5$) to temperature changes is because of the fact that they are thinner and respond faster to changes in thermal conductivity compared to the inner regions of the disk ($r/R < 0.5$) which are bulkier.

As observed from the plotted results (Figure 15) the increase in thermal conductivity has an inverse impact on the disk temperature gradients over the inner and outer regions of the rotating disk. This reversal of the thermal trend is observed at 80 percent ($r/R = 0.8$) of the normalized disk radius(Figure 15). The increase in the thermal conductivity benefits the very outer regions of the disk near the shroud ($r/R > 0.8$) by lowering the temperature gradients which can be critical in enhancing the life of the compressor disks as the highest gradients as seen from the plot (Figure 15) are experienced near the shroud. But on the contrary increase in the thermal conductivity raises the temperature gradients over the majority of the disk which are below 80 percent ($r/R < 0.8$) of it’s normalized radius which if not within the limits can over run the advantage gained in the outer regions resulting in the lowering of the disk operating life.Also as observed from the table of results (Table 5) the temperature gradients towards the middle of the disk ($r / R = 0.5$)are more sensitive (56 percent) to changes in the thermal conductivity compared to the inner and outer regions of the rotating compressor disk. Overall the analysis reveals that the increase in thermal conductivity benefits only the very outer regions of the disk by lowering the temperature gradients and on the contrary raises the temperature gradients over the majority of the disk.

VII. IMPACT OF DISK THICKNESS ON THE DISK TEMPERATURE GRADIENTS

The Ansys thermal model which is validated with the “Test and Measurement Conditions” (Table 1) is used to investigate the impact caused by the changes in the disk thickness t (Figure 1) on the disk temperature gradients. The radial heat conduction (Q_y) through a disk thickness t and at a radius r from the rotational axis is given by equation 23. With reference to this equation 23 for the ease of modelling instead of changing the thickness t in the Ansys geometry the thermal conductivity of the disk material along the radial direction (K_y) is varied keeping the axial thermal conductivity (K_x) constant as shown in table 6. The changes in the disk thickness t can hence be effectively modelled by proportionately varying radial thermal conductivity (K_y) treating the disk material as polytropic.

$$Q_y = - K_y(2\pi r t) (dt/dy) \tag{23}$$

Table .6Modelling the changes in the disk thickness by varying the radial thermal conductivity

Disk Tickness (mm)	% increase in thickness	Thermal Conductivity (K_x) W/m K	Thermal Conductivity (K_y) W/m K
10.80	Base model thickness	11	11.00
12.96	20 % increase in thickness	11	13.20
15.12	40 % increase in thickness	11	15.40
17.28	60 % increase in thickness	11	17.60

Figure 16 shows the temperature distribution on the rotating disks obtained from Ansys for the minimum ($t = 10.8$ mm) and the maximum ($t = 17.28$ mm) thickness of the compressor disk under study.

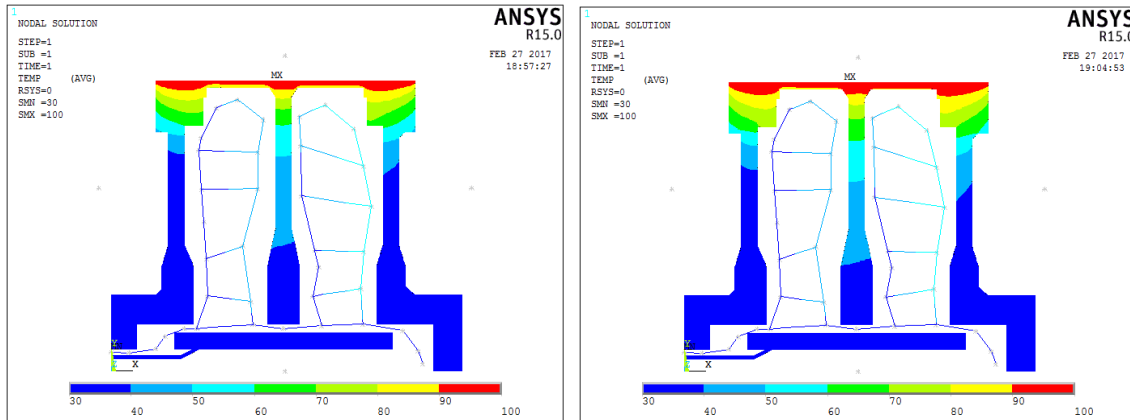


Fig.16 Ansys plot of temperature distribution for the minimum ($t = 10.8$ mm) and the maximum ($t = 17.28$ mm) disk thickness.

Figure 17 shows the temperatures and the temperature gradients along the mid-section (Figure 4) of the rotating compressor disk for the different thickness of the disks. The vertical scale of the plot represents the disk local radius r which is normalized with the disk outer radius R . The horizontal scale represents the disk nodal temperatures and disk nodal temperature gradients estimated using the Ansys simulation. Tables 6 and 7 show the percentage change in disk temperatures and disk temperature gradients estimated at different radial locations of the disk as the thickness of the disk is increased from the minimum ($t = 10.8 \text{ mm}$) to the maximum ($t = 17.28 \text{ mm}$).

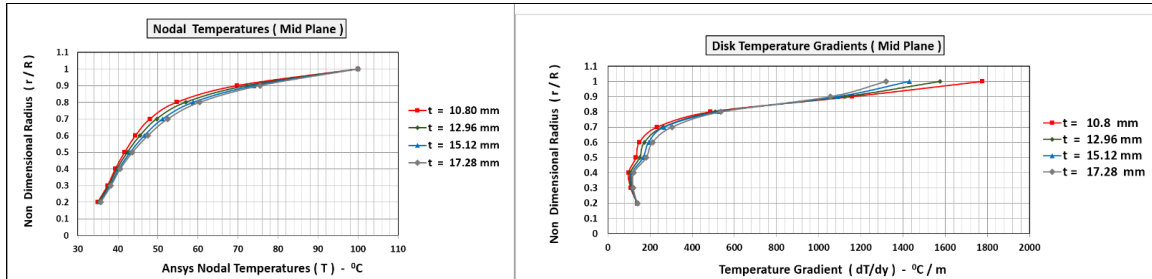


Fig.17 Impact of changes in disk thickness on the disk temperatures and the disk temperature gradients

Table .6 Impact of disk thickness on temperatures

Disk Radial Location (r/R)	Disk Temperature °C		% change in temperature
	$t = 10.8 \text{ mm}$	$t = 17.28 \text{ mm}$	
0.2	35	36	3
0.4	39	41	5
0.6	44	47	7
0.8	55	60	9
0.9	70	75	7

Table .7 Impact of disk thickness on temperature gradients

Disk Radial Location (r/R)	Disk Temperature Gradient °C/m		% change in Temperature Gradient
	$t = 10.8 \text{ mm}$	$t = 17.28 \text{ mm}$	
0.2	139	140	1
0.4	98	123	26
0.6	149	212	42
0.8	486	535	10
0.9	1157	1056	-9

As seen from the Ansys temperature contours (Figure 16) and the plotted results (Figure 17) the increase in the disk thickness raises the disk temperatures over the entire disk from its inner to the outer radii. Also as seen from figure 17 and table 6 the changes in the disk thickness have a more significant impact on the disk temperatures towards its outer regions ($r/R > 0.5$) compared to its inner regions.

As observed from the plotted results (Figure 17) the increase in the disk thickness has an inverse impact on the disk temperature gradients over the inner and the very outer regions of the rotating disk. This reversal of the thermal trend is observed at 90 percent ($r/R = 0.9$) of the normalized disk radius (Figure 17). The increase in the disk thickness benefits the very outer regions ($r/R > 0.9$) by lowering the disk temperature gradients. As seen from the gradient plot (Figure 17) the maximum temperature gradients exist towards these very outer regions and the reductions in the temperature gradients achieved in these regions by increasing the thickness would be critical in enhancing the operating life of the disks. On the contrary the increase in the disk thickness has an adverse impact over the regions of the disk which are below 90 percent of the normalized radius ($r/R < 0.9$) by increasing the temperature gradients. As observed from table 7 the maximum impact of change in the thickness on the temperature gradients is felt towards the middle regions of the disk ($r/R = 0.5$). Based on the above observations it is hence recommended to make efforts to reduce the thickness of the disk except on its very outer regions ($r/R > 0.9$) where on the contrary it is recommended to increase the thickness to lower the disk temperature gradients. Efforts need to be focused on reducing the temperature gradients near the shroud ($r/R > 0.9$) as these regions experience the maximum thermal stresses and are hence critical in the design for enhancing the operating life of these disks.

Figure 19 shows the temperature distribution on the rotating compressor disks obtained from Ansys for the minimum (20%) and the maximum (50%) of the through flow that enters into the rotor cavity.

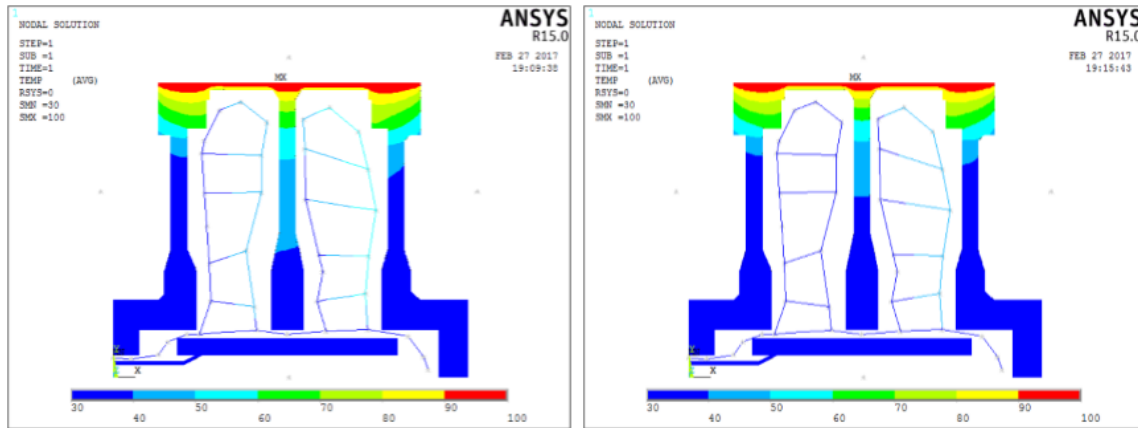


Fig.19 Ansys plot of temperature distribution for the minimum (20%) and the maximum (50%) percentage of the through flow entering cavity.

Figure 20 shows the temperatures and the temperature gradients along the mid-section (Figure 4) of the rotating compressor disk for the different percentages of the through flow entering the disk cavity. The vertical scale of the plot represents the disk local radius r which is normalized with the disk outer radius R . The horizontal scale represents the disk nodal temperatures and disk nodal temperature gradients estimated using the Ansys simulation. Tables 8 and 9 show the percentage change in disk temperatures and disk temperature gradients estimated at different radial locations of the disk as the percentage of the through flow that circulates into the cavity is increased from the minimum (20%) to the maximum (50%).

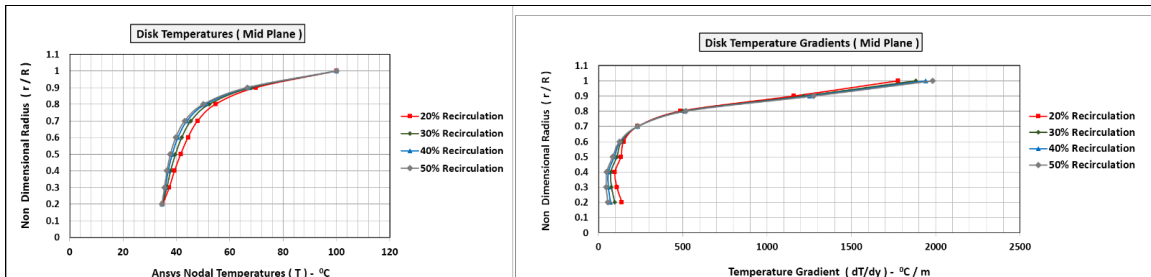


Fig.20 Impact of changes in percentage of through flow into cavity on the disk temperatures and the disk temperature gradients

Table .8 Impact of percentage flow circulation on disk temperatures

Disk Radial Location (r/R)	Disk Temperature °C		% change in temperature
	20% Circulation	50% Circulation	
0.2	35	35	0
0.4	39	36	-8
0.6	44	40	-9
0.8	55	50	-9
0.9	70	67	-4

Table .9 Impact of percentage flow circulation on disk temperature gradients

Disk Radial Location (r/R)	Disk Temperature Gradient °C / m		% change in Temperature Gradient
	20% Circulation	50% Circulation	
0.2	139	55	-60
0.4	98	49	-50
0.6	149	125	-16
0.8	486	518	7
0.9	1157	1275	10

As seen from the Ansys contours (Figure 19) and the plotted results of temperature distribution (Figure 20) the increase in the percentage of the through flow entering the disk cavity lowers the disk temperatures. This impact of the flow circulation on the lowering the disk temperatures is more significant (9 percent) towards the outer regions ($0.6 < r/R < 0.9$) of the rotating disk (Table 8) compared to the inner regions. This is on account of the following two features which dominate in the outer regions. 1) Owing to the flow pattern (Figure 18) the flow in the outer regions is cooler than the inner regions (Figure 19) permitting greater rates of heat transfer compared to the inner regions. 2) The mass of the circulating flow that interacts with the rotating disk is higher in the outer regions compared to the inner regions of the rotating disk (Figure 18).

As observed from the temperature gradient plot (Figure 20) the changes in the percentage of through flow entering the cavity has an inverse impact on the disk temperature gradients over its inner and the outer regions. This reversal of the thermal trend is observed at 70 percent ($r/R = 0.7$) of the normalized disk radius (Figure 20). The increase in the percentage of the through flow entering the cavity benefits the majority of the disk ($r/R < 0.7$) by lowering the disk temperature gradients. This lowering of the temperature gradients is more prominent towards the inner regions ($r/R < 0.2$) of the disk compared to the middle regions (Table 9). At the very inner region ($r/R = 0.2$) the reduction in the temperature gradient is 60 percent compared to 16 percent at the middle region of the disk ($r/R = 0.5$) as recorded in table 9. The outer regions of the disk which are over 70 percent ($r/R > 0.7$) of the normalized disk radius experience a rise in the temperature gradients with increasing percentage of the through flow entering the disk cavity (Figure 20). This rise in the temperature gradient is more prominent (10%) towards the shroud ($r/R > 0.9$) compared to the other outer regions of the disk (Table 9).

Overall the analysis reveals that increasing the percentage of the through flow entering the cavity benefits the majority of the disk ($r/R < 0.7$) by reducing the temperature gradients thereby offering benefits of enhancements to the operating life of the compressor disks. But design alternatives need to be considered for the very outer regions ($r/R > 0.7$) of the disk which experience rise in the temperature gradients with increasing percentage of the through flow entering the cavity. One of the design alternative is to increase the disk thickness gradually towards the shroud which would counter the above effect by lowering the temperature gradients in the outer regions as reported in the outcomes of section 7. As the regions near the shroud experience the highest temperature gradients (Figure 20) reducing the temperature gradients in the outer regions of the disk is critical in enhancing the operating life of the compressor disks.

The increase in the percentage of the through flow entering the cavity that reduces the temperature gradients over the majority of the disk can be achieved by designing and operating the compressor disks with a smaller Rossby number RO_{ax} and a larger axial gap ratio G . This in the design can be achieved by (referring to figure 1)

Decreasing the axial flow velocity ($V_{ax,in}$) at the inlet

Increasing the rotational speed (ω) of the disks

Increasing the axial spacing (s) between the adjacent disks

Decreasing the outer radius (R_b) of the rotating cavity.

IX. CONCLUSIONS

The operating life of the compressor disks of an aircraft engine is greatly influenced by the temperature gradients it experiences during its field operations. It hence becomes critically important to design the compressor disks and the secondary flow system which minimize these temperature gradients experienced by the high speed rotating compressor disks. Owing to the complexity of the thermal fluid behaviour and the range of inter dependent factors effecting the disk temperatures it is almost impractical to perform experiments for a wide range of design configurations. Hence it becomes necessary to conduct numerical estimations of the heat transfer and the fluid flow characteristics after these computer models have been duly validated with the experimental data. The impact of the disk design and the disk material on the temperature gradients of these compressor disks is investigated with the aid of computer aided simulations carried out using computational fluid dynamics (CFD) and finite element analysis (FEA). The computer models built for this study are validated with the engine experimental data. The investigation also deals with the parametric impact of the design changes on the various thermal fluid parameters in the secondary flow system, the convective heat transfer coefficients and the rate of heat generation in the disk cavities that ultimately influence the temperature gradients over the compressor disks. In the later part of this report (Sections 6, 7, 8) the impact of the changes in the disk design and the disk material on the disk temperature gradients is analysed and reported based on the estimated results. The various outcomes coming out of this investigation and the recommendations offer support in the design and development of the aircraft engine compressor disks aimed at lowering the disk temperature gradients. The reductions achieved in the disk temperature gradients would help in enhancing the operating life of the compressor and at the same time help in lowering the maintenance cost of these widely used aero engines.

X. ACKNOWLEDGMENTS

I would like to acknowledge the necessary support provided by Osmania University and C.B.I.T for the successful execution and completion of this research work.

XI. REFERENCES

- [1] A. Günther, W. Uffrecht, L. Heller, S. Odenbach, “Experimental and Numerical Analysis of Heat Transfer in Compressor Disc Cavities for a transition between Heating and Cooling Flow”, 8th ETC, Graz, 111, 2009.
- [2] Sparrow, E. M., Leonardo Goldstein Jr “Effect of Rotation and Coolant Through Flow on the Heat Transfer and Temperature Field in an Enclosure, J. Heat Transfer, 98, pp. 387-394, 1976
- [3] Farthing, P. R., Long, C. A., Owen, J. M., Pincombe, J. R., “Rotating Cavity with Axial Through Flow of Cooling Air: Heat Transfer”, J. Turbomach., 114, pp. 229–236 , 1992.
- [4] Farthing, P. R., Long, C. A., Owen, J. M., Pincombe, J. R., “Rotating Cavity with Axial Through Flow of Cooling Air: Flow Structure”, ASME J. Turbomach., 114, pp. 237–246,1992.
- [5] S. Seghir-Ouali a, “Convective Heat Transfer Inside a Rotating Cylinder with an Axial Air Flow”, International Journal of Thermal Sciences, 45, pp. 1166–1178, 2006.
- [6] C. Gazley, Jr., “Heat Transfer Characteristics of the Rotation and Axial Flow between Concentric Cylinders , ASME Trans., 80, pp.79-90, 1958.
- [7] S. Harmand, J. Pelle, S. Poncet , I.V. Shevchuk , “Review of Fluid Flow and Convective Heat Transfer within Rotating Disk Cavities with Impinging Jet”, International Journal of Thermal Sciences, 67, pp.1-30, 2013.
- [8] Lloyd, J.R., Moran, W.R., “Natural Convection Adjacent to Horizontal Surfaces of Various Planforms”, ASME Paper 74-WA/HT- 66, 1974.
- [9] CP Kothandaraman , S Subramanyan, “Heat and Mass Transfer Data”, Fourth edition, New Age International Publishers. pp.116-117.
- [10] Owen, J. M., and Pincombe, J. R., “Vortex Breakdown in a Rotating Cylindrical Cavity,” J. Fluid Mech., 90, pp. 109–127, 1979.
- [11] Roland Wiberg , Noam Lior, “Heat Transfer from a Cylinder in Axial Turbulent Flows”, International Journal of Heat and Mass Transfer, 48, pp.1505–1517, 2005.
- [12] Sparrow, E. M., Buszkiewicz, T. C., and Eckert, E. R. G., “Heat Transfer And Temperature Field Experiments In A Cavity With Rotation, Recirculation And Coolant Through Flow,” J. Heat Transfer, 97(1), pp. 22-28, 1975.
- [13] C. A. Long and P. G. Tucker, “Shroud Heat Transfer Measurements from a Rotating Cavity with an Axial Through flow of Air”, J. Turbomach 116 (3), pp..525-534, 2015.
- [14] Dr. K.E. Reby Roy and K. Madhusoodanan Pillai, “Flow and Conjugate Heat Transfer Characteristics in a Rotating Disk Cavity with Through-Flow”, International Journal of Applied Engineering Research, 7 (12), pp. 1429-1441, 2012.
- [15] C. A. Long, “Disk Heat Transfer in a Rotating Cavity with an Axial Through Flow of Cooling Air”, Int. J. Heat and Fluid Flow, 15 (4), pp. 307-316, August 1994.
- [16] J. Michael Owen, Jonathan Powell, “Buoyancy-Induced Flow in a Heated Rotating Cavity”, Transactions of the ASME, 128, January 2006.
- [17] Dayle C. Jogie, “The Study of Fluid Flow and Heat Transfer of a Viscous Incompressible Fluid Between a Rotating Solid Disk and a Stationary Permeable Disk Using the Brinkman-Darcy Model”, Journal of Applied Mathematics and Mechanics, 96(5), pp. 620-632, 2016..
- [18] X. Luo, L. Wang, X. Zhao, G. Xu, H. Wu, “Experimental Investigation of Heat Transfer in a Rotor–Stator Cavity with Cooling Air Inlet at Low Radius”, International Journal of Heat and Mass Transfer, 76, pp.65-80, 2014.
- [19] Xiang Luo, L. Wang, “Experimental Investigation of Heat Transfer in a Rotor–Stator Cavity with Cooling Air Inlet at Low Radius, International Journal of Heat and Mass Transfer”, 76, pp.65–80, 2014.
- [20] D.A. Howey a, A.S. Holmes a , K.R. Pullen b, “Radially Resolved Measurement of Stator Heat Transfer in a Rotor–Stator Disc System”, International Journal of Heat and Mass Transfer, 53, pp.491–501, 2010.
- [21] M.M. Rahman, J.C. Lallave, A. Kumar, “Heat Transfer from a Spinning Disk during Semi–Confined Axial Impingement from a Rotating Nozzle”, Int. J. Heat Mass Transfer, 51, 4400–4414, 2008.
- [22] R. P. Roy, G. Xu, J. Feng, “A Study of Convective Heat Transfer in a Model Rotor–Stator Disk Cavity”, J. Turbomachinery, 123(3), pp.621-632, 2001.